Tbx1 regulates fibroblast growth factors in the anterior heart field through a reinforcing autoregulatory loop involving forkhead transcription factors

Tonghuan Hu[1,2,*], Hiroyuki Yamagishi[1,2,3,*], Jun Maeda[1,2,*], John McAnally[2], Chihiro Yamagishi[1,2,3] and Deepak Srivastava[1,2,†]

[1]Department of Pediatrics, University of Texas Southwestern Medical Center, Dallas, TX 75390-9148, USA
[2]Department of Department of Molecular Biology, University of Texas Southwestern Medical Center, Dallas, TX 75390-9148, USA
[3]Department of Pediatrics, Keio University School of Medicine, 35 Shinanomachi, Shinjuku-ku, Tokyo 160-8582, Japan
*These authors contributed equally to this work
†Author for correspondence (e-mail: deepak.srivastava@utsouthwestern.edu)

Summary

Birth defects, which occur in one out of 20 live births, often affect multiple organs that have common developmental origins. Human and mouse studies indicate that haploinsufficiency of the transcription factor TBX1 disrupts pharyngeal arch development, resulting in the cardiac and craniofacial features associated with microdeletion of 22q11 (del22q11), the most frequent human deletion syndrome. Here, we have generated an allelic series of *Tbx1* deficiency that reveals a lower critical threshold for Tbx1 activity in the cardiac outflow tract compared with other pharyngeal arch derivatives, including the palatal bones. Mice hypomorphic for Tbx1 failed to activate expression of the forkhead transcription factor Foxa2 in the pharyngeal mesoderm, which contains cardiac outflow precursors derived from the anterior heart field. We identified a Fox-binding site upstream of *Tbx1* that interacted with Foxa2 and was necessary for pharyngeal mesoderm expression of *Tbx1*, revealing an autoregulatory loop that may explain the increased cardiac sensitivity to Tbx1 dose. Downstream of Tbx1, we found a fibroblast growth factor 8 (Fgf8) enhancer that was dependent on Tbx1 in vivo for regulating expression in the cardiac outflow tract, but not in pharyngeal arches. Consistent with its role in regulating cardiac outflow tract cells Tbx1 gain of function resulted in expansion of the cardiac outflow tract segment derived from the anterior heart field as marked by Fgf10. These findings reveal a Tbx1-dependent transcriptional and signaling network in the cardiac outflow tract that renders mouse cardiovascular development more susceptible than craniofacial development to a reduction in Tbx1 dose, similar to humans with del22q11.

Key words: Tbx1, 22q11.2 deletion syndrome, Anterior heart field, Foxa2, Fgf8, Fgf10

Introduction

Human chromosomal deletion syndromes are common causes of birth defects, but the complex and rare nature of such deletions have made a mechanistic analysis of the developmental anomalies elusive. 22q11.2 deletion syndrome (22q11DS), the most common genetic deletion syndrome in human, is typically characterized by heterozygous microdeletion of a 1.5 to 3 Mb region of chromosome 22q11.2 (Shaikh et al., 2001). 22q11DS, which includes DiGeorge syndrome (DGS), velocardiofacial syndrome (VCFS) and conotruncal anomaly face syndrome, is characterized by a broad spectrum of phenotypic abnormalities, including cardiac defects, abnormal facies, thymic hypoplasia, cleft palate and hypocalcemia (Lindsay, 2001; Scambler, 2000). Although the clinical features are highly variable and affect many organs, structures primarily affected in 22q11DS are derivatives of the pharyngeal apparatus, suggesting that defects in pharyngeal development cause most features of this disease (Epstein, 2001; Yamagishi and Srivastava, 2003).

The pharyngeal apparatus is a transient vertebrate-specific complex that arises from a series of bilaterally symmetric bulges on the ventrolateral surface of the head and neck region, namely the pharyngeal arches. The arches develop in a cranial-caudal sequence under the control of clustered homeobox (Hox) genes and are composed of a number of different embryonic cell types (Graham, 2003; Graham and Smith, 2001). Distinct lineages within the pharyngeal arches serve as precursors to a wide variety of cardiac and craniofacial structures, including those derived from pharyngeal endoderm, ectoderm, mesoderm and neural crest mesenchyme. Paracrine signaling between each group of cells reciprocally regulates cell fate, proliferation and death decisions. Arterial vessels arising from the heart traverse symmetrically through each pharyngeal arch and are ultimately patterned along the cranial-caudal axis in an intricate fashion to form the mature aortic arch and pulmonary artery. Neural crest-derived cells are involved in the patterning of these vessels and in septation of the single cardiac outflow tract into two distinct vessels (Yutzey and Kirby, 2002).

A more recently recognized lineage involving the pharyngeal arches is the anterior or secondary heart field (Mjaatvedt et al., 2001; Waldo et al., 2001; Kelly et al., 2001). In contrast to the atrial and ventricular chambers that arise from lateral cardiac mesoderm progenitors, the most anterior pole of the heart comprising the outflow tract and part of the right ventricle is added later by mesodermal cells in the pharyngeal region that lie anterior and dorsal to the heart tube. The anterior heart field cells are thought to migrate into the outflow tract through the pharyngeal mesoderm, which also contributes to facial muscles (Lu et al., 2002), and differentiate into myocardium and endocardium. The regulatory processes that govern its development remain largely unknown, although fibroblast growth factor 10 (Fgf10) and the transcription factor Islet1 mark these cells and are involved in their development (Kelly et al., 2001; Cai et al., 2004).

Because the cardiac outflow tract is the predominant region affected in 22q11DS, this syndrome may afford an opportunity to understand development of the anterior heart field and its role in the outflow tract. Tbx1, a member of the T-box-containing family of transcription factors, is the most likely candidate gene within the 22q11 locus responsible for the pharyngeal arch-derived defects observed (Lindsay et al., 1999; Lindsay et al., 2001; Merscher et al., 2001; Schinke and Izumo, 2001). Mice heterozygous for targeted deletion of *Tbx1* have a low penetrance (25%) of aortic arch patterning defects, but little evidence of other features of 22q11DS (Lindsay et al., 2001; Merscher et al., 2001). By contrast, homozygous-null mutants of *Tbx1* have most features of 22q11DS, including absence of thymus, cleft palate, ear defects and characteristic cardiac outflow tract anomalies (Jerome and Papaioannou, 2001). Correspondingly, *Tbx1* is expressed in the pharyngeal arch endoderm, mesodermal core, anterior heart field and head mesenchyme, although it is conspicuously absent in the neural crest-derived mesenchyme (Chapman et al., 1996; Garg et al., 2001; Yamagishi et al., 2003). We have previously shown that *Tbx1* is regulated by a sonic hedgehog signaling cascade that is directly mediated by a conserved Fox-binding site upstream of *Tbx1* that directs *Tbx1* expression in the pharyngeal endoderm and head mesenchyme (Yamagishi et al., 2003). However, the cell types through which Tbx1 functions, its downstream targets and its regulation in the pharyngeal mesoderm/anterior heart field remain unknown.

As *Tbx1* is a dose-dependent gene and the dose can probably be affected by genetic and environmental modifiers, we have generated an allelic series of *Tbx1* deficiency in an attempt to recapitulate more accurately the human del22q11 phenotype and to determine the domains of *Tbx1* expression that regulate crucial developmental events. The data presented here suggest that development of the cardiac outflow tract is more sensitive to *Tbx1* allelic dose than the craniofacial region, and that this may be due to a reinforcing autoregulatory loop involving transcription factor, Foxa2, in the pharyngeal mesoderm precursors of the outflow tract. *Tbx1* transcripts were selectively downregulated in the pharyngeal mesoderm but not endoderm of *Tbx1* hypomorphic mutants. We also found that *Foxa2* transcription was diminished specifically in the pharyngeal mesoderm of the *Tbx1* hypomorphic mutant and that a Fox site was essential for regulation of *Tbx1* in the pharyngeal mesoderm, suggesting that a Tbx1-Foxa2 pathway amplifies *Tbx1* expression in the mesoderm. A genome-wide

search for Tbx1 targets in the heart identified a cardiac outflow tract enhancer sufficient for fibroblast growth factor 8 (Fgf8) expression that was regulated by Tbx1 in vivo. Moreover, misexpression of Tbx1 in the developing heart resulted in expansion of the outflow tract, as marked by the secondary heart field marker, Fgf10. These findings demonstrate an essential role for Tbx1 in regulating the pharyngeal mesoderm through an amplification loop involving forkhead proteins and culminating in regulation of fibroblast growth factors in the cardiac outflow tract, consistent with the increased allelic dose sensitivity to Tbx1 in the outflow tract compared to the craniofacial region.

Materials and methods

Generation of Tbx1 deficient mice

The targeting construct used to create a hypomorphic and conditional deletion allele of Tbx1 was generated as follows. The Frt-flanked neomycin resistant gene (NEO) driven by the PGK promoter was inserted in an intron between exon 3 and exon 4 of *Tbx1*. A 3.5 kb homologous region containing exon 4 to exon 8 was inserted between two loxP sites in order to remove the entire T-box region after Cre-recombinase expression. Embryonic stem (ES) cells were screened by Southern blot and the targeted clones were injected into mouse blastocysts. Germline transmission of hypomorphic alleles ($Tbx1^{neo}$) was obtained by mating chimeric mice with C57BL6 mice to produce 129×C57BL6 mixed background F1 mice, and with 129SvEv mice to produce 129 inbred mice. F1 heterozygous mice ($Tbx1^{neo/+}$) were intercrossed to produce F2 offspring for analysis. Germline transmission of the targeted allele from two independent ES cell clones was obtained and the phenotype of the animals from these two lines was undistinguishable. Heterozygous mice ($Tbx1^{neo/+}$) were also mated with MORE (Mox2Cre) mice to ubiquitously delete exons 4-8, resulting in the heterozygous *Tbx1* null allele ($Tbx1^{+/-}$). Genotyping was performed by Southern analysis or PCR of genomic DNA extracted from yolk sac for embryos or tail for neonatal pups.

RT-PCR

Total RNA was isolated from E10.0 embryos with Trizol reagent (Gibco BRL) according to the manufacturer's instruction. Total RNA (1 μg) was reverse-transcribed with M-MuLV reverse transcriptase by a random primer labeling method (Roche). RT product (2 μl) was amplified with primers 5′-GCGCTGTGGGACGAGTTCAATCAG-3′ (from exon 3) and 5′-GCACAAAGTCCATGAGCAGCATGTAGTC-3′ (from exon 4) for 36 cycles to detect *Tbx1* cDNA, or with primers 5′-ACCACAGTCCATGCCATCAC-3′ and 5′-TCCACCACCCTG-TTGCTGTA-3′ for 30 cycles to detect GAPDH control cDNA.

Cartilage and skeletal preparation

Standard methods were followed for Alcian Blue cartilage preparations and Alizarin Red for skeletal preparations.

Radioactive section in situ hybridization

^{35}S-labeled antisense riboprobes were synthesized with T3, T7 or SP6 RNA polymerse (MAXIscript in vitro transcription kit, Ambion, Austin, TX) from capsulin, Dlx2, Foxc1, Foxc2, Bmp7, Hand2, Et1, Fgf10, Foxa2, Nkx2.6, Pax1, Pax9, Tbx1 or Fgf8 cDNAs. Radioactive section in situ hybridizations were performed on paraffin wax-embedded sections of E9.25 to E10.5 wild type, hypomorphic mutant ($Tbx1^{neo/neo}$), null mutant ($Tbx1^{-/-}$) or compound mutant ($Tbx1^{neo/-}$) mouse embryos as previously described (Thomas et al., 1998). Sources of DNAs for making probes were as follows: Foxc1, Foxc2, Foxa2 and Tbx1 (Yamagishi et al., 2003); Dlx2, Hand2 and Et1 (Thomas et al., 1998); Fgf8 (Meyers and Martin, 1999); Fgf10 (Kelly et al., 2001); capsulin (Lu et al., 2002); Bmp7, Nkx2.6, Pax1 and Pax9

full-length cDNAs were cloned by RT-PCR amplification from mouse E9.5 RNA. In situ hybridization of probes shown were performed at least three times on different embryos.

Generation of transgenic mice

A 5.4 kb DNA fragment (–5406/–18) upstream of the Fgf8 start codon was amplified from human genomic DNA by PCR using primers 5′-CCTGTGCTGGGTGATGTTTCCCTAG-3′ and 5′-ACCGAGA-GCCCGGCGGGTCACGC-3′. This fragment and its derivatives were cloned into an hsp68-lacZ reporter construct (Kothary et al., 1989). Mothers were sacrificed at E9.5 and F0 embryos were stained for β-galactosidase (β-gal) activity. Stable transgenic lines were established with a minimal 0.9kb (–5406/–4510) fragment. Potential Tbx-binding sites within this region included the following sequences: GGTGGGA, –5208/–5202; TCAGCACT, –5149/–5143; TGTGAGG, –4948/–4942; GGTGACA, –4925/–4919; GGTGGCC, –4902/–4896. Similar studies were performed with genomic DNA upstream of *Tbx1*. Site-directed mutagenesis was used to create point mutations of Fox site upstream of *Tbx1* as described previously (Yamagishi et al., 2003).

Tbx1 cDNA was cloned downstream of the β-myosin heavy chain promoter and linearized plasmid was injected into pronuclei to generate F0 transgenic embryos with Tbx1 expression throughout the embryonic myocardium.

Results

Dose sensitivity of Tbx1 in a tissue-specific fashion

Mice heterozygous for *Tbx1* have a mild, incompletely penetrant phenotype, while homozygous null animals suffer severe defects of the pharyngeal arch-derived craniofacial and cardiac regions. In order to study the mechanisms of Tbx1 dose sensitivity in its many expression domains, we engineered a hypomorphic allele of *Tbx1* that was used to generate an allelic series of Tbx1 dose. We inserted the neomycin resistance gene in the intronic region between exons 3 and 4 of mouse *Tbx1* by homologous recombination ($Tbx1^{neo/+}$) and placed loxP sites around exons 4 and 8. Ubiquitous cre-recombinase mediated excision resulted in a *Tbx1* heterozygous-null allele ($Tbx1^{+/-}$) (Fig. 1). A series of matings was performed to
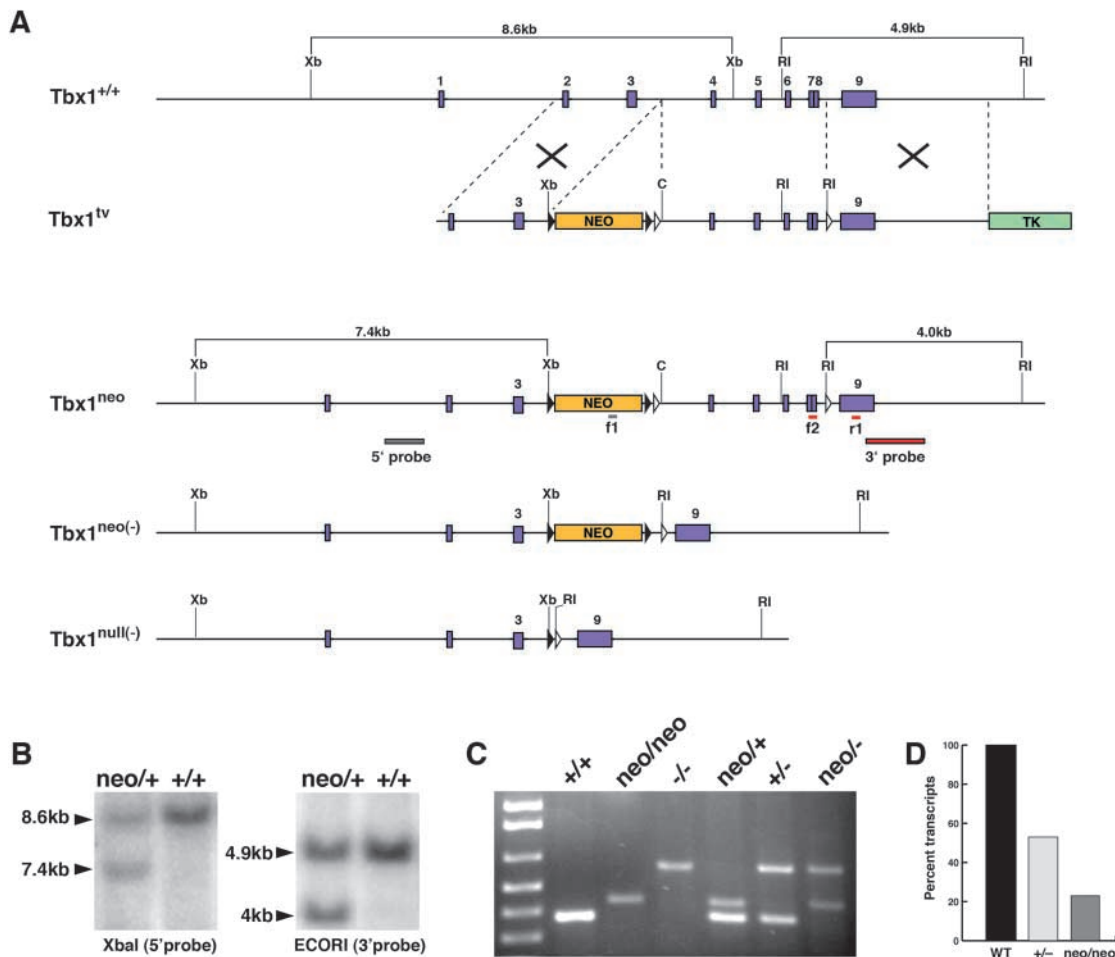
Fig. 1. Generation of *Tbx1* hypomorphic and null alleles. (A) Targeting strategy. Tbx1$^{+/+}$, wild-type allele; Tbx1^{tv}, targeting vector; Tbx1^{neo}, hypomorphic allele; Tbx1$^{neo(-)}$, null allele with neo; Tbx1$^{null(-)}$, null allele without neo. Exon numbers and restriction enzyme sites (C, *Cla*I; RI, *Eco*RI; Xb, *Xba*I) are indicated. White triangles represent Cre-recombinase sites; black triangles are FLP-recombinase sites. (B) Southern analysis of genomic DNA from ES cell clones after digestion with *Xba*I and *Eco*RI and hybridizing with 5′ and 3′ probes, respectively, which demonstrate targeted event (neo/+) compared with wild-type allele (+/+). (C) PCR genotyping analysis of various *Tbx1* alleles with forward (f1,f2) and reverse (r1) primers. +/+, *Tbx1* wild type; neo/neo, *Tbx1* hypomorphic homozygous; –/–, *Tbx1*-null; neo/+, *Tbx1* hypomorphic heterozygous; +/–, *Tbx1* heterozygous; neo/–, *Tbx1* compound mutant mice. (D) Quantification of Tbx1 mRNA transcripts detected by RT-PCR in heterozygous and hypomorphic E10.5 mouse embryos compared with wild type set at 100%.
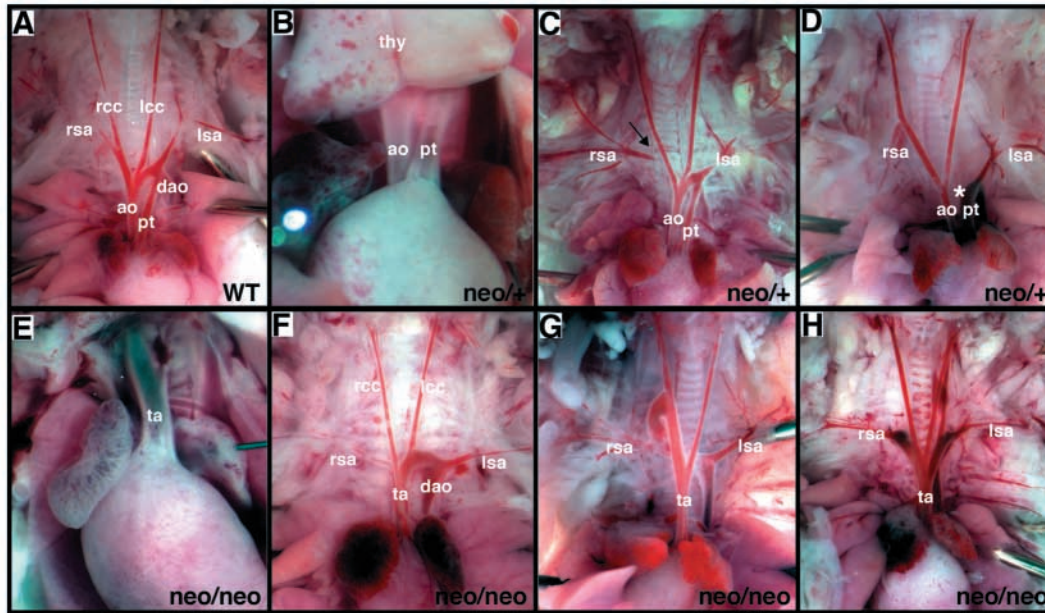
Fig. 2. Cardiovascular and thymic defects in *Tbx1* hypomorphic mutant neonates. Frontal views of heart and vessels in *Tbx1* hypomorphic heterozygous (*Tbx1neo/+*) neonates (B-D), and in *Tbx1* hypomorphic homozygous (*Tbx1neo/neo*) neonates (E-H). (A) Wild-type neonate with thymus removed to illustrate normal septation of outflow tract into aorta (ao) and pulmonary trunk (pt), and patterning of the aortic arch with the right subclavian artery (rsa), right common carotid artery (rcc), left common carotid artery (lcc), left subclavian artery (lsa) and descending aorta (dao). (B) *Tbx1neo/+* neonate had normal development of thymus (thy) and normal anatomy of great vessels with the aorta located to the right and dorsal to the pulmonary trunk. (C,D) Thymus was removed to visualize arch anatomy. (C) *Tbx1neo/+* mice displayed aberrant origin of right subclavian artery (rsa) with it seen traversing behind the trachea (arrow) to connect to the dao. (D) Interruption of the aortic arch with no connection between the ascending and descending aorta (*).(E-H) Majority of *Tbx1neo/neo* neonates had persistent truncus arteriosus (ta) that resulted from failure of aorto-pulmonary septum formation. In addition, aplasia of the thymus occurred with complete penetrance. Exposure of the aortic arch in *Tbx1neo/neo* mice revealed a variety of aortic arch patterning defects in conjunction with persistent truncus arteriosus, including aberrant origin of the dao from the carotid (G), and abnormal origins of the carotid arteries and lsa (H).

generate *Tbx1neo/neo*, *Tbx1neo/–* and *Tbx1–/–* mice in mixed (129sv/C57BL6) and pure genetic backgrounds (129sv). RT-PCR from E10.0 embryos revealed that *Tbx1neo/neo* embryos generated ~25% *Tbx1* mRNA compared with wild-type (*Tbx1+/+*) littermates (Fig. 1D), suggesting that insertion of *Neo* in *Tbx1* intron 3 resulted in significant reduction of *Tbx1* mRNA production, similar to that previously described for *Fgf8* (Meyers et al., 1998).

Mice heterozygous for the hypomorphic allele (*Tbx1neo/+*) had ~2% neonatal lethality caused by interruption of the aortic arch and nearly 10% incidence of aberrant origin of the right subclavian artery, both of which are defects of the fourth pharyngeal arch arteries (Fig. 2C,D). *Tbx1* heterozygous (*Tbx1+/–*) mutants had similar aortic arch defects compared with *Tbx1neo/+* mutants but had a higher penetrance, resulting in nearly 10% neonatal lethality and 20% incidence of arch

anomalies (summarized in Table 1). By contrast, 100% of animals homozygous for the hypomorphic allele (*Tbx1neo/neo*) died immediately after birth with a spectrum of birth defects that were overlapping but distinct from *Tbx1–/–* newborns. The majority had a persistent truncus arteriosus (PTA) and ventricular septal defect (VSD), reflecting failure of septation of the primitive conotruncal vessel into the ascending aorta and main pulmonary artery. However, a few newborns had malalignment of the outflow tract, resulting in both vessels arising from the right ventricle [double-outlet right ventricle (DORV)]. All *Tbx1neo/neo* mutants with PTA had an aberrant right subclavian artery with a variety of aortic arch patterning defects, including right-sided and double aortic arches (Fig. 2F-H). Further reduction of *Tbx1* in compound mutant (*Tbx1neo/–*) mice resulted in 100% penetrance of PTA and arch anomalies in mixed or pure genetic backgrounds and the

Table 1. Summary of developmental defects in Tbx1 neonatal mutant mice

Genotype	Number of embryos	Cardiovascular defects				Cranial facial defects		Aplasia of thymus
		PTA	DAA	ARSC	IAA-B	Absent ears	Cleft palate	
neo/+	81	0 (0%)	0 (0%)	6 (7%)	2 (2%)	0 (0%)	0 (0%)	0 (0%)
+/–	37	0 (0%)	0 (0%)	5 (14%)	3 (8%)	0 (0%)	0 (0%)	0 (0%)
neo/neo	39	35 (90%)	2 (5%)	35 (90%)	2 (5%)	0 (0%)	0 (0%)	39 (100%)
neo/–	14	14 (100%)	0 (0%)	14 (100%)	0 (0%)	14 (100%)	7 (50%)	14 (100%)
–/–	19	18 (95%)	1 (5%)	18 (95%)	0 (0%)	19 (100%)	19 (100%)	19 (100%)

PTA, persistent truncus arteriosus; DAA, double aortic arch; ARSC, Aberrant right subclavian artery; IAA-B, interrupted aortic arch type B.

cardiovascular phenotype was indistinguishable from *Tbx1* homozygous-null (*Tbx1⁻/⁻*) mutants described here and previously (Jerome and Papaioannou, 2001). Presence of the neo cassette did not influence gene expression of other candidate genes in the region, including *Ufd1*, *Crkl* or *Gscl* (data not shown). Thus, progressive depletion of *Tbx1* transcripts resulted in increasing severity of cardiovascular malformations with a 75% reduction being sufficient to cause most of the cardiovascular features observed in complete nulls.

A subset of pharyngeal arch derivatives is Tbx1 dose-sensitive

Although the cardiac defects were severe in *Tbx1^neo/neo^* mutants, most derivatives of the pharyngeal arches were normal in mice with the hypomorphic allele. Exceptions to this included the complete aplasia of the endodermally derived thymus, which occurred with 100% penetrance in hypomorphic mice. In addition, ear anomalies, which are common in 22q11DS, were observed with varying severity in the different allelic dosages of Tbx1. The first and second pharyngeal arches contribute to the external and middle ear structures, while the inner ear arises from the otic vesicle. In *Tbx1^neo/neo^* mutants the external ears, stapes (bone of middle ear) and inner ear were smaller than wild type but not as severely affected as the null mutants, where the structures were essentially absent (Fig. 3A-F). The tympanic ring was also progressively smaller. Finally, non-pharyngeal arch derived bones of the basal skull (basioccipital and basisphenoid bones), were abnormally fused in both *Tbx1^neo/neo^* mutants and *Tbx1⁻/⁻* mutants (Fig. 3G-I).

In contrast to the sensitivity of the cardiovascular system and certain pharyngeal arch derivatives, palatal development was relatively unaffected by incremental reductions in *Tbx1* dose. Bilateral palatine shelves, outgrowths from the maxillary prominences of the first pharyngeal arch, normally migrate to the midline and fuse, resulting in separation of the oral and nasal cavities. In our *Tbx1⁻/⁻* mutants, the palatine shelves failed to fuse, resulting in a cleft palate (Fig. 3G-I), similar to previous reports. However, all *Tbx1^neo/+^* and *Tbx1^neo/neo^* mutants had fusion of the palatine shelves, resulting in normal formation of the palate (Fig. 3K). Thus, unlike the cardiac defects, a reduction in *Tbx1* dose up to 25% of normal had no effect on palate development.

Similar to the palate, most derivatives of the pharyngeal arches, other than those described above, were not as sensitive to the dose of Tbx1 as was the cardiovascular system. Cartilage and skeletal preparation from neonatal animals showed that first pharyngeal arch derivatives, including maxillary, zygomatic and temporal bones appeared grossly normal in hypomorphic mutants (*Tbx1^neo/neo^*) when compared with wild-type or *Tbx1^neo/+^* littermates (Fig. 3J-L). By contrast, these structures were condensed and abnormal in null mutants (*Tbx1⁻/⁻*). The second, third, fourth and sixth pharyngeal arches form various cartilage structures in the neck region, such as hyoid bone, thyroid cartilage and cricoid cartilage. In *Tbx1^neo/neo^* mutants, all neck cartilage structures developed normally with the exception that a component of the hyoid bone was missing. By comparison, the cartilages of the neck were small and fragmentary structures in *Tbx1⁻/⁻* mutants (Fig. 3J-L). Thus, most pharyngeal arch mesenchyme derivatives
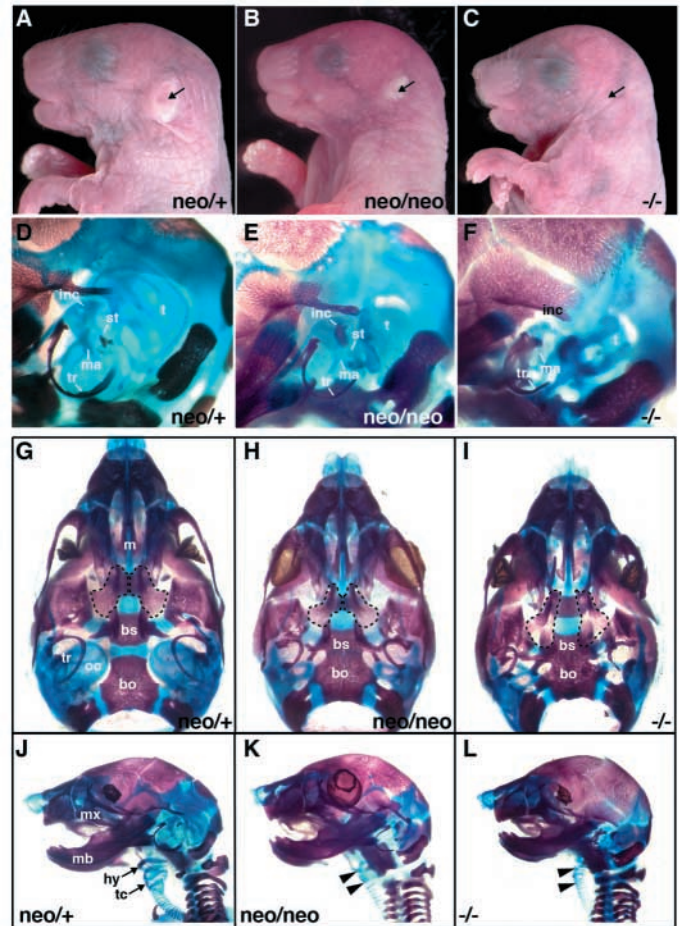
Fig. 3. Ear and craniofacial defects in *Tbx1* hypomorphic (*neo/neo*) and null (–/–) mutants. (A-C) Left lateral views revealed that *Tbx1^neo/neo^* mutants (B) had smaller but normal shaped ears (arrows) compared with *Tbx1^neo/+^* (A), which was similar to wild type. *Tbx1⁻/⁻* mutants (C) showed absent external ears. (D-F) Left-sided views of skeletal preparations of neonatal skulls focusing on ear region (blue or red indicates cartilage or bone, respectively). The malleus (ma) and incus (inc) middle ear structures were progressively hypoplastic in the *Tbx1^neo/neo^* (E) and *Tbx1⁻/⁻* (F) mutants compared with *Tbx1^neo/+^* (D). The stapes (st), was hypoplastic in *Tbx1^neo/neo^* mutants and was absent in *Tbx1⁻/⁻* mutants. The cartilage primordium of petrous part of the temporal bone (t) also exhibited a gradient of hypoplasticity with progressive reduction in Tbx1 dose. (G-I) Ventral view of skull skeletal preparations demonstrated that both *Tbx1^neo/neo^* mutants (H) and *Tbx1⁻/⁻* mutants (I) had abnormal fusion of the basioccipital (bs) and basisphenoid (bo) bones. However, cleft palate was present only in *Tbx1⁻/⁻* mutants, caused by failure of fusion of the palatine shelves outlined by broken lines. The otic capsule (oc), an inner ear structure, also exhibited severe hypoplasticity in both *Tbx1^neo/neo^* mutants and *Tbx1⁻/⁻* mutants. (J-L) Left lateral views of skeletal preparations of the face and neck. *Tbx1^neo/neo^* (K) and *Tbx1⁻/⁻* (L) mutants failed to form the body of the hyoid bone (hy) in the neck. The rest of the neck cartilage structure (arrowheads), such as thyroid cartilage (tc) appeared normal in *Tbx1^neo/neo^* mutants, but was reduced to small and fragmentary structures in *Tbx1⁻/⁻* mutants (L). m, maxillary shelves; mx, maxilla; mb, mandible; tr, tympanic ring.

were not affected by reduction of *Tbx1* dose, resulting from the hypomorphic allele.

Tissue-specific effects of Tbx1 alleles on Tbx1 and Foxa2 transcript levels

To understand the mechanisms through which *Tbx1* hypomorphic alleles affected some tissues more than others, we examined the *Tbx1* transcript level in specific expression domains, including the head mesenchyme, pharyngeal mesoderm and pharyngeal endoderm, as previously described (Garg et al., 2001). Coronal sections of E9.5 *Tbx1^neo/neo* embryos revealed that *Tbx1* expression was nearly abolished in the outflow precursors of the pharyngeal mesoderm and reduced in head mesenchyme, but was remarkably conserved in pharyngeal endoderm. These observations were consistent with the tissue-specific allelic dose-sensitivity described above and may explain the more severe cardiovascular dose-sensitivity of *Tbx1* hypomorphs. As expected, *Tbx1* expression was undetectable in *Tbx1^-/-* embryos (Fig. 4A-C).

To investigate the underlying basis for tissue-specific regulation and function in the *Tbx1* hypomorphic allele, we examined the effects of *Tbx1* transcript levels on a variety of pharyngeal mesoderm and endoderm markers. As expected from the relatively normal level of Tbx1 transcripts in the *Tbx1^neo/neo* pharyngeal endoderm, the expression of *Pax1*, a paired-box-containing gene that is normally expressed in the pharyngeal endoderm at E9.5 (Muller et al., 1996), was unaffected in the hypomorphic mutant. *Pax1* expression was also robust in the endoderm of *Tbx1^-/-* mutants in spite of the pharyngeal arch segmentation defect (Fig. 4D-F), as was

expression of additional endodermal markers, including Pax9 and Nkx2.6 (Biben et al., 1998; Muller et al., 1996) (data not shown). Markers of the neural crest-derived mesenchyme, including Dlx2 and Hand2 were also normal (Thomas et al., 1998) (Fig. 4G-I and data not shown).

Because *Tbx1* expression in the pharyngeal mesoderm was selectively extinguished in the *Tbx1^neo/neo* mice, we investigated the effects on other genes expressed in this cell type. Expression of the pharyngeal mesoderm marker, capsulin 1 (Lu et al., 2002), indicated that pharyngeal mesodermal cells were present in the *Tbx1* hypomorph and null embryos (Fig. 4J-L). Upon examination of numerous other candidate genes, we found that *Foxa2*, which encodes a forkhead-containing transcription factor, was expressed at high levels in the pharyngeal mesoderm in addition to its known endodermal expression. However, in the *Tbx1* hypomorph and in the null mutants, *Foxa2* was selectively downregulated in the pharyngeal mesoderm and head mesenchyme, but not in the endoderm (Fig. 4M-O). These results are consistent with the more prominent cardiac outflow tract phenotype in the *Tbx1* hypomorphic state as the pharyngeal mesoderm cells give rise to the most anterior pole of the heart comprising the outflow tract.

Foxa2 regulates Tbx1 in the pharyngeal mesoderm

Our group has previously demonstrated that the forkhead-containing transcription factors Foxc1 and Foxc2 directly
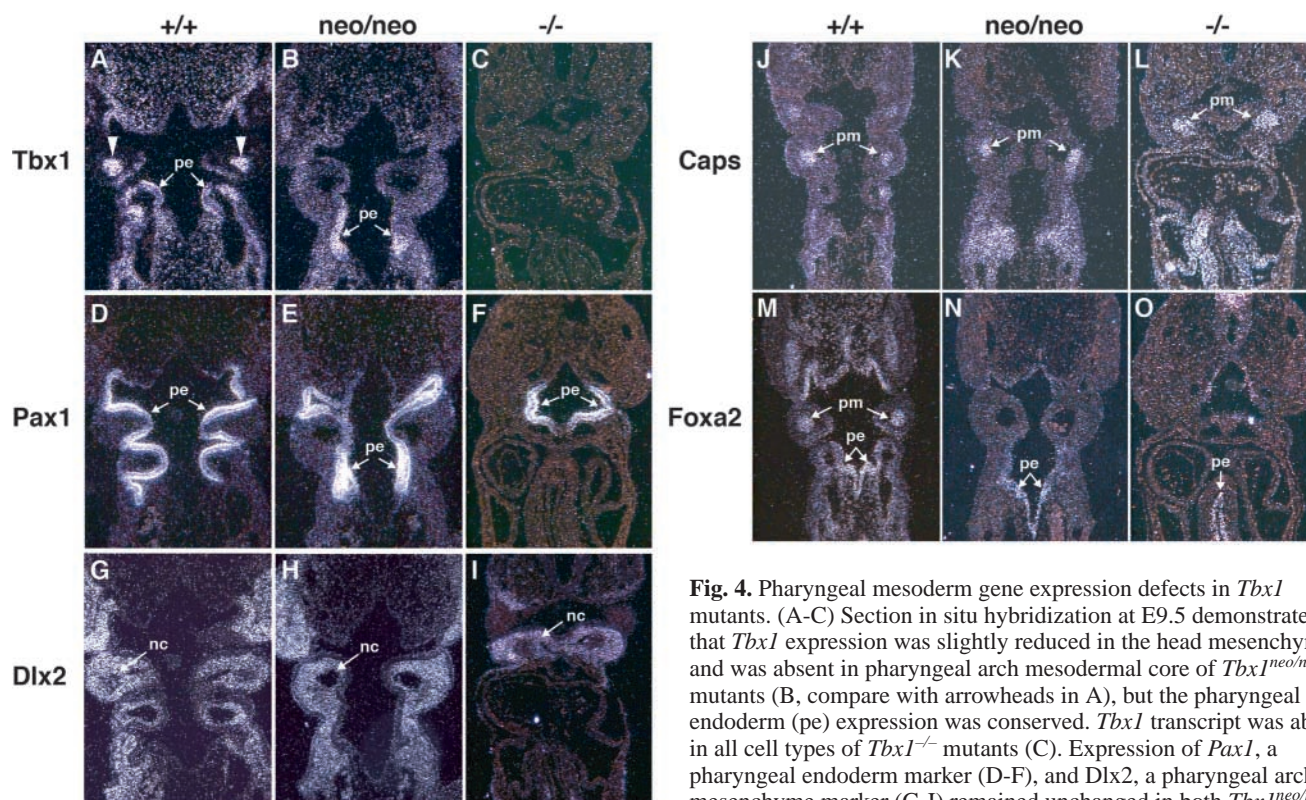
Fig. 4. Pharyngeal mesoderm gene expression defects in *Tbx1* mutants. (A-C) Section in situ hybridization at E9.5 demonstrated that *Tbx1* expression was slightly reduced in the head mesenchyme and was absent in pharyngeal arch mesodermal core of *Tbx1^neo/neo* mutants (B, compare with arrowheads in A), but the pharyngeal endoderm (pe) expression was conserved. *Tbx1* transcript was absent in all cell types of *Tbx1^-/-* mutants (C). Expression of *Pax1*, a pharyngeal endoderm marker (D-F), and Dlx2, a pharyngeal arch mesenchyme marker (G-I) remained unchanged in both *Tbx1^neo/neo* mutants (E,H) and *Tbx1^-/-* mutants (F,I). (J-L) Capsulin (Caps) was expressed normally in the pharyngeal mesoderm (pm) core in both *Tbx1^neo/neo* mutants (K) and *Tbx1^-/-* mutants (L) when compared with the wild-type littermates. (M-O) In adjacent sections from the same embryo, *Foxa2* expression in pharyngeal endoderm was largely conserved, but expression in the pharyngeal mesoderm core was completely missing in both mutants (N,O). Results shown are representative of at least three separate experiments.

regulated *Tbx1* in the head mesenchyme, and that Foxa2 regulated *Tbx1* expression in the pharyngeal endoderm (Yamagishi et al., 2003). However, we had not isolated any specific cis elements that consistently regulated *Tbx1* in the pharyngeal mesoderm or cardiac outflow tract. Because *Tbx1* expression was selectively downregulated in the pharyngeal mesoderm of *Tbx1* hypomorphic mice, and due to the importance of this cell type in cardiac outflow tract development, we sought to determine the mechanism through which *Tbx1* regulation might be selectively affected in the mesoderm. A 12.8 kb genomic fragment extending 14.3 kb upstream of the translational start site of *Tbx1* is capable of recapitulating all of the Tbx1 expression domains including the mesoderm (Fig. 5A,B) (Yamagishi et al., 2003). We generated a series of genomic fragments within the 12.8 kb region upstream of a basal promoter and a *lacZ* reporter and injected these fragments into pronuclei to search for a *Tbx1* mesoderm enhancer (Fig. 5). Using VISTA software to compare genomic regions conserved across species, we identified regions of high homology between human and mouse that contained conserved cis elements. One of these regions, encompassing 1.5 kb, could direct pharyngeal mesoderm and cardiac outflow tract expression (Fig. 5E-H), but only in conjunction with the previously described 200 bp fragment containing a Fox site essential for endoderm and head mesenchyme expression

(Yamagishi et al., 2003). A point mutation of the Fox site in the context of the 200 bp and 1.5 kb fragments ablated the endodermal and head mesenchyme expression, and also disrupted pharyngeal mesoderm and outflow tract expression (Fig. 5). These results suggest that the Fox site in the distal enhancer is necessary for directing pharyngeal mesoderm expression, but requires a second enhancer for high-level expression in this domain. By electromobility shift assay, Foxa2 and Foxc1/2 can bind and activate transcription through this site (Yamagishi et al., 2003). Because we show here that Foxa2 is expressed in the pharyngeal mesoderm and is downregulated in the *Tbx1* hypomorphic mutant, it may function in a reinforcing loop that amplifies *Tbx1* expression in the pharyngeal mesoderm but not endoderm, potentially explaining the lower levels of *Tbx1* transcripts in the pharyngeal mesoderm of the hypomorphic embryos and the more dose-sensitive phenotype in mesodermal derivatives. Whether Foxc1/2 can play such a role in the outflow tract or even in the pharyngeal mesoderm remains to be determined.

Outflow tract regulation of Fgf8 is disrupted in Tbx1 mutant mice

To determine how Tbx1 may regulate pharyngeal arch development, we sought to identify Tbx1 target genes by searching the mouse genome for consensus T-box binding sites
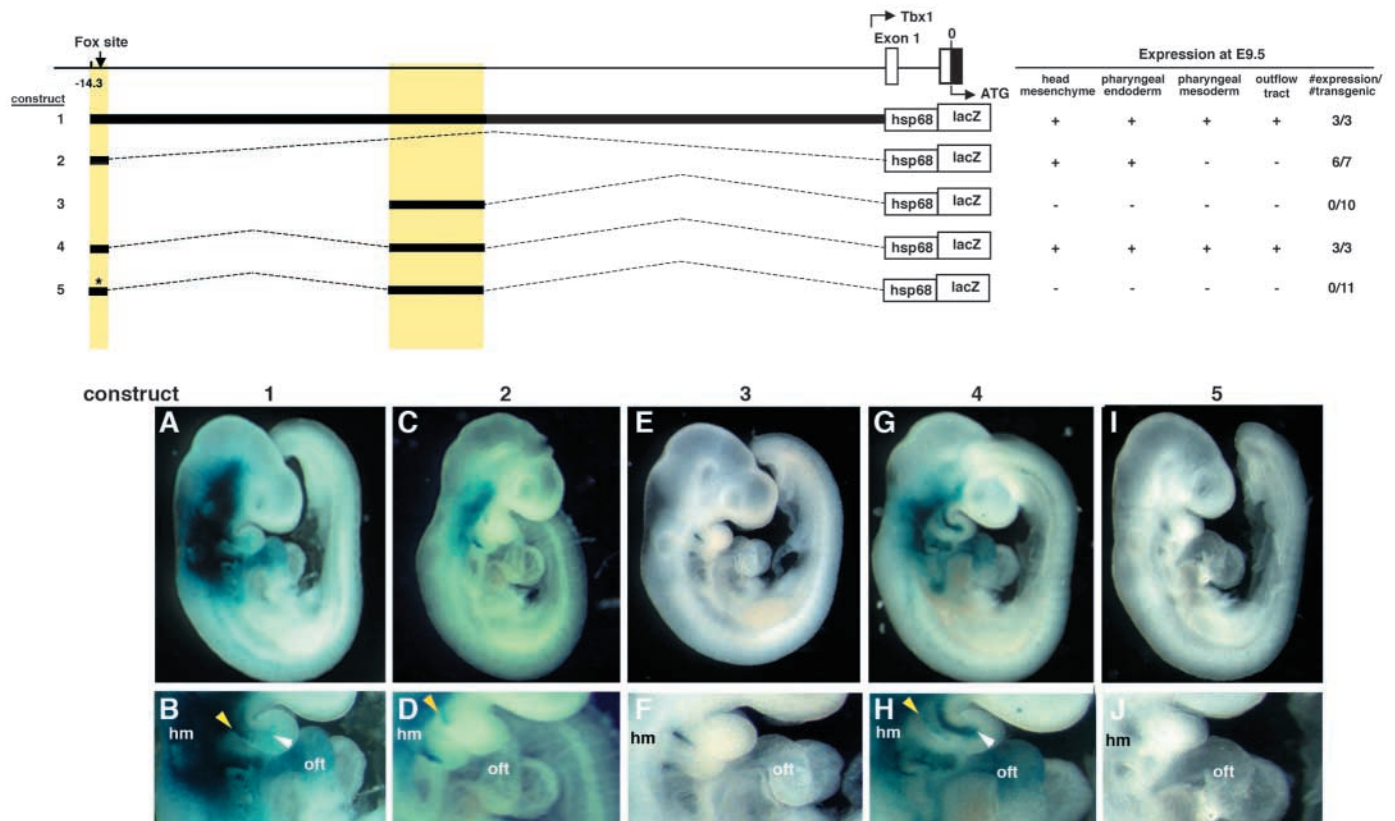

Fig. 5. Fox cis element is necessary for pharyngeal mesoderm and cardiac outflow expression of *Tbx1*. (Upper panel) Genomic organization of the 5′ mouse *Tbx1* locus. Boxes indicate exons, and the translation start site (ATG) is designated as nucleotide number zero. Construct number is indicated on the left, and the corresponding expression pattern of *lacZ* is summarized on the right. Mutation of Fox site is indicated by star. (A,C,E,G,I), Right lateral view of representative embryos obtained with indicated constructs; (B,D,F,H,J) magnified right lateral views of above focused on pharyngeal arch and outflow tract region. Pharyngeal mesoderm (white arrowheads), pharyngeal endoderm (yellow arrowheads), cardiac outflow tract (oft) and head mesenchyme (hm) expression is evident.

located within 10 kb upstream of known genes. From this list, we focused on ten genes that were reportedly expressed in the pharyngeal arches and we cloned the conserved T-box-containing genomic regions upstream of luciferase reporters. All potential enhancer-luciferase plasmids were transfected into COS1 cells with or without Tbx1 to determine if Tbx1 was directly capable of activating transcription in vitro. Of the ten candidates, only one, the enhancer of fibroblast growth factor

8 (Fgf8), was activated by Tbx1 in vitro. Previous studies showed that the *Fgf8* hypomorphic mutant phenocopied many features of 22q11DS, and suggested that *Fgf8* might act downstream of Tbx1 in the pharyngeal endoderm (Abu-Issa et al., 2002; Frank et al., 2002; Vitelli et al., 2002; Brown et al., 2004). In an attempt to determine whether *Fgf8* might act as a direct downstream target of Tbx1, we isolated a 5.4 kb DNA fragment (–5406/–18) 5′ of the *Fgf8* start codon (Fig. 6). This

fragment and its derivatives were subcloned upstream of a *lacZ* reporter gene. Mouse embryos harboring this transgene consistently showed β-gal staining in the pharyngeal endoderm and ectoderm at E9.5, recapitulating endogenous *Fgf8* expression (Crossley and Martin, 1995). In addition, the transgene directed *lacZ* expression in the cardiac outflow tract in all transgenic lines, highly similar to *Tbx1* transgene expression (Fig. 6B). The cardiac outflow tract expression has not previously been reported, but we were able to detect Fgf8 transcripts in this domain by RNA in situ hybridization (Fig. 6C), similar to the cardiac outflow tract expression of *lacZ* upon insertion of a *lacZ* cassette into the *Fgf8* locus under control of endogenous *Fgf8* regulatory elements (E. Meyers, personal communication). Interestingly, lacZ expression was also seen in the pharyngeal mesoderm, which contributes to the cardiac outflow tract (Fig. 6B).

To localize the regulatory elements responsible for expression of *Fgf8*, we generated a series of deletions in the 5.4 kb genomic fragment and analyzed their ability to drive *lacZ* expression from a heterologous promoter (*hsp68*) in F0 transgenic mice at E9.5 (Fig. 6). Comparison of the sequences that directed appropriate *Fgf8* expression revealed that a 0.9 kb distal fragment containing many conserved core T-box binding sequences was
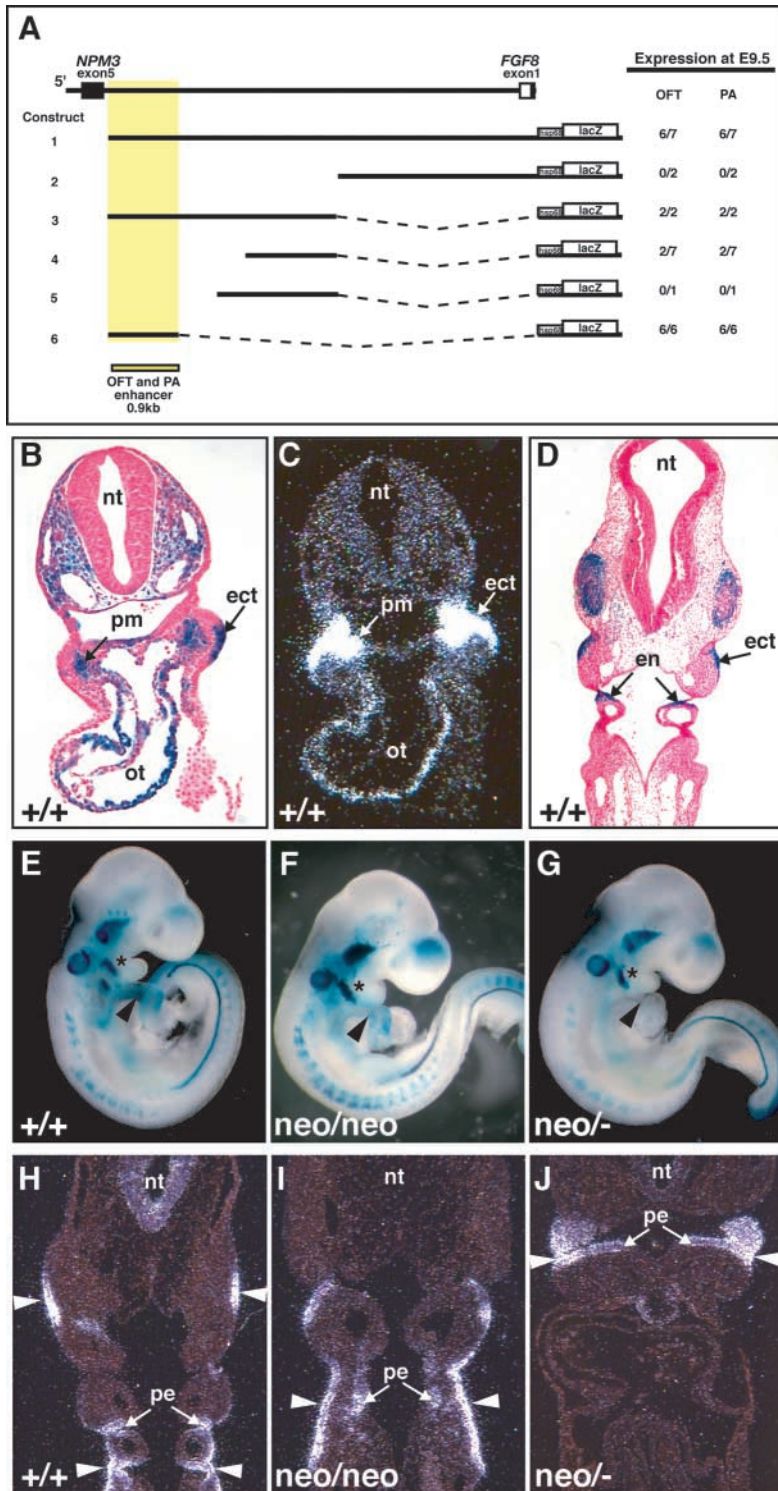
Fig. 6. Identification of regulatory regions for *Fgf8* expression in pharyngeal arches and the outflow tract. (A) Genomic organization of the 5′ mouse *Fgf8* locus. Construct number is indicated on the left, and the corresponding expression pattern of *lacZ* in the outflow tract (OFT) or pharyngeal arch (PA) is summarized on the right. (B,C) Transverse sections of E9.5 transgenic mice (construct 6) stained for *lacZ* (B) or section in situ hybridization for Fgf8 transcripts (C) showing cardiac outflow tract (ot) and pharyngeal mesoderm (pm) expression. nt, neural tube. (D) Coronal section of transgenic mice made with construct 6 showing pharyngeal endoderm (pe) and ectoderm (ect) expression. (E) Right lateral view of representative E9.5 embryo obtained with stable transgenic line made with construct 6 showing pharyngeal arch (*) and cardiac outflow tract (black arrowhead) *lacZ* expression. (F,G) *Fgf8-lacZ* transgenic line from (E) in *Tbx1*[neo/neo] or *Tbx1*[neo/–] genetic background. Black arrowhead indicates progressive decrease in outflow tract expression. (H-J) Coronal section in situ hybridization of E10.0 embryos with Fgf8 probe indicates preserved ectodermal (white arrowheads) and pharyngeal endoderm (pe) expression of *Fgf8* in *Tbx1*[neo/neo] or *Tbx1*[neo/–] embryos. *Tbx1*^{–/–} embryos were identical to *Tbx1*[neo/–] in phenotype and gene expression.

sufficient to drive *Fgf8* expression in the pharyngeal endoderm, ectoderm and cardiac outflow tract (Fig. 6B). These T-box binding sites were defined by a core sequence as previously described (Conlon et al., 2001) (see Materials and methods). To determine if the *Fgf8* upstream region was Tbx1-sensitive in vivo, we generated stable mouse lines of the *Fgf8* enhancer driving *lacZ* and intercrossed these mice with *Tbx1*$^{neo/+}$ mice to ultimately generate *Fgf8*^{lacZ} *Tbx1*$^{neo/neo}$ and *Fgf8*^{lacZ} *Tbx1*$^{neo/-}$ embryos. Mice lacking *Tbx1* did not have any *Fgf8* downregulation in the pharyngeal endoderm or ectoderm, but the cardiac outflow tract expression was reduced in *Tbx1*$^{neo/neo}$ embryos and undetectable in the *Tbx1*$^{neo/-}$ embryos (Fig. 6E-G). This was also true for the *Tbx1*$^{-/-}$ mutants. The lack of pharyngeal arch downregulation was consistent with our results by RNA in situ hybridization (Fig. 6H-J) in which endoderm and ectoderm expression of *Fgf8* was preserved in the absence of Tbx1, suggesting that the cardiac outflow tract was the major site of Tbx1-Fgf8 regulation.

Tbx1 regulation of the anterior heart field

Because *Tbx1* was expressed in splanchnic mesoderm that gives rise to anterior heart field cells as early as the cardiac crescent stage (Yamagishi et al., 2003), and Tbx1 later regulated *Fgf8* in the outflow tract derived from this domain, we tested whether Tbx1 was required for *Fgf8* or *Fgf10* expression in the anterior heart field cells dorsal to the heart in the pharyngeal region. By sagittal sectioning, we found that *Tbx1* expression was decreased in the anterior heart field in the *Tbx1*$^{neo/neo}$ background (Fig. 7A). *Fgf8* and *Fgf10* expression was detected in this domain but was selectively diminished in the *Tbx1*$^{neo/neo}$ background (Fig. 7B,C, arrowheads) consistent with Tbx1-mediated regulation of Fgf genes in the anterior heart field and cardiac outflow tract. Similar results were

observed in *Tbx1*$^{-/-}$ mice (data not shown). To test in vivo whether Tbx1 was sufficient to activate Fgf gene expression, we mis-expressed *Tbx1* throughout the developing mouse myocardium using the β-myosin heavy chain promoter, disrupting its normal restriction to the cardiac outflow tract myocardium. *Tbx1* mis-expressing mice were found to have an elongated outflow tract at E10.5, suggesting that *Tbx1* misexpression resulted in an expansion of outflow tract myocardium or reprogramming of ventricular cardiomyocytes into outflow tract cells. Analysis of the elongated outflow tract using Fgf8 and Fgf10, as a marker of the anterior heart field revealed that this expanded domain was indeed characteristic of anterior heart field cells (Fig. 7C; data not shown). Disruption of cardiac development induced by Tbx1 misexpression resulted in embryonic death precluding examination of the effects on outflow septation or alignment.

Discussion

Here, we have shown that cardiogenesis is more sensitive than facial development to *Tbx1* allelic disruption and that this sensitivity is probably explained by selectively reduced *Tbx1* mRNA in pharyngeal mesoderm of *Tbx1* hypomorphic mutants. We provide evidence that *Foxa2* is selectively downregulated in pharyngeal mesoderm of *Tbx1*$^{neo/neo}$ embryos and also show that a Fox site is necessary for pharyngeal mesoderm and cardiac outflow tract expression of *Tbx1* in vivo. These observations suggest an autoregulatory loop involving forkhead proteins that may normally amplify the Tbx1 signal in pharyngeal mesoderm. Within the outflow tract, we obtained in vivo evidence that *Fgf8* requires Tbx1 for its expression in the cardiac outflow tract but that Tbx1 was dispensable for pharyngeal endoderm and ectoderm expression of *Fgf8*.
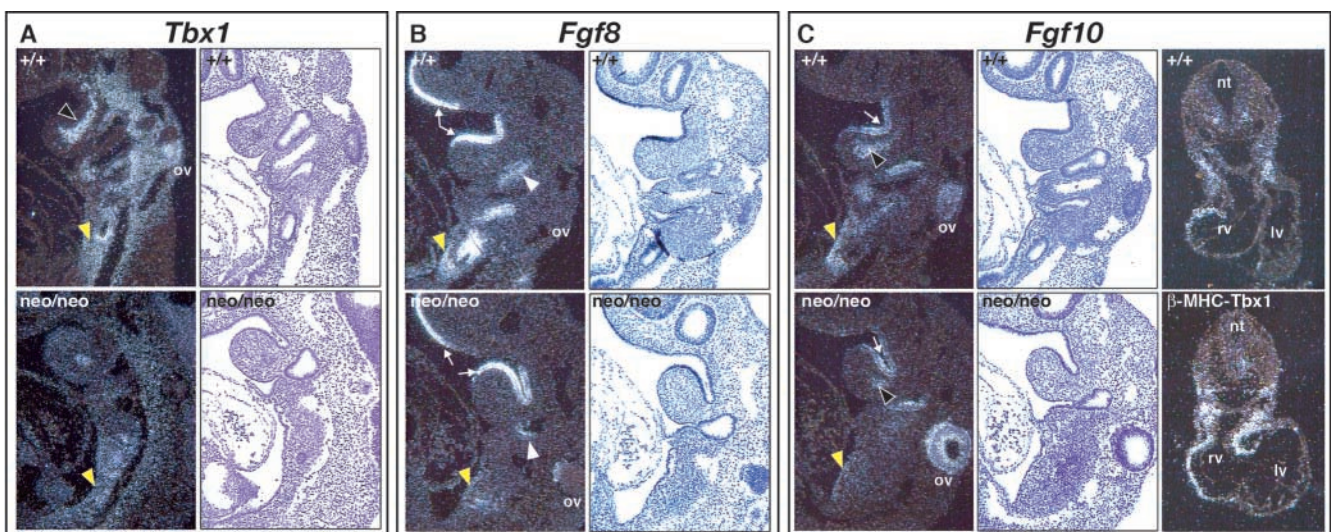
Fig. 7. Tbx1 and fibroblast growth factors in anterior heart field. (A) Sagittal section in situ hybridization of E9.5 embryos with Tbx1 (A), Fgf8 (B) or Fgf10 (C) riboprobes on wild-type (+/+, top row) or *Tbx1*$^{neo/neo}$ embryos (bottom row) focusing on pharyngeal arch region. Pharyngeal mesoderm that is probably in the anterior heart field dorsal to the heart is indicated by yellow arrowheads. Black arrowheads indicate pharyngeal core mesoderm expression; white arrowheads indicate pharyngeal endoderm; white arrows indicate pharyngeal ectoderm. *Fgf8* and *Fgf10* are downregulated in areas marked by yellow arrowheads in *Tbx1*$^{neo/neo}$ embryos. Bright-field images are shown. Right-most panels in C represent transverse sections through the cardiac outflow tract of E9.5 wild-type (+/+) embryos or transgenic embryos misexpressing *Tbx1* in the heart under control of the β-MHC promoter (β-MHC-Tbx1). The domain of *Fgf10* expression was expanded in transgenic mice, as detected by in situ hybridization. ov, otic vesicle; rv, right ventricle; lv, left ventricle; nt, neural tube.

Finally, a positive role for Tbx1 in either activating anterior heart field gene expression or its domain is provided by gain-of-function experiments demonstrating expansion of Fgf10-expressing cells in the heart. Together, this work provides multiple avenues of evidence that Tbx1 is essential for normal cardiac outflow tract development via its pharyngeal mesoderm/anterior heart field domain of expression.

Cardiovascular dose-sensitivity to Tbx1

Based on the near complete penetrance of persistent truncus arteriosus in $Tbx1^{neo/neo}$ embryos but 0% incidence of cleft palate or absent ears, the cardiovascular system appeared to be more sensitive to the dose of *Tbx1* than did parts of the craniofacial region. Aortic arch patterning was even more sensitive, with defects observed in $Tbx1^{neo/+}$ mice. This is consistent with clinical observations where ~75% of 22q11DS have cardiac defects but only 30% have cleft palate. However, our work could suggest that the embryonic regions may not be differentially sensitive to *Tbx1* mRNA levels but rather more sensitive to some allelic alterations. The evidence for this comes from the observation that the *Tbx1* mRNA levels were not equal in the various expression domains of $Tbx1^{neo/neo}$ mice but rather was more severely affected in the pharyngeal mesoderm. This would explain the more severe phenotype in pharyngeal mesoderm-derived cells, such as the anterior heart field cells of the cardiac outflow tract. Based on these data, it is possible that in humans, heterozygosity of *TBX1* results in differential levels of *TBX1* mRNA levels in its diverse expression domains, thereby resulting in varying incidence of disease in specific organs with or without genetic modifiers or stochastic events.

Pharyngeal mesoderm transcription of Tbx1 is affected by a Fox-mediated autoregulatory loop

The selective mesoderm decrease in *Tbx1* mRNA levels described above was an unexpected but interesting result. The expression of *Foxa2* in the pharyngeal mesoderm was also a surprise as we and others have considered *Foxa2* a more endoderm-specific gene, at least in the pharyngeal arches. The observation that *Foxa2* was downregulated in the pharyngeal mesoderm but not endoderm of $Tbx1^{neo/neo}$ mice provided an opportunity to understand the mechanism that might potentially explain the mesoderm-specific decrease in *Tbx1* mRNA in $Tbx1^{neo/neo}$ mice. Because we show that a Fox site is necessary for pharyngeal mesoderm and cardiac outflow tract expression of *Tbx1* in transgenic mice, it is possible that Foxa2 may be the trans-acting factor that regulates *Tbx1* in the pharyngeal mesoderm. Evidence to support this is that Foxa2 can bind the essential Fox site and activate transcription through it (Yamagishi et al., 2003). In addition, *Foxa2* expression in the mesoderm overlaps *Tbx1* more closely than any other Fox protein to our knowledge. Unfortunately, *Foxa2* mutant mice die very early, prior to a time at which we could test whether Foxa2 is necessary for *Tbx1* transcription in the pharyngeal mesoderm (Ang and Rossant, 1994; Weinstein et al., 1994). Therefore, we must still consider the possibility that other forkhead-containing proteins might be involved in *Tbx1* regulation in this domain. For example, *Foxc2* is expressed in the cardiac outflow tract (Winnier et al., 1999; Kume et al., 2001) and could also be regulating *Tbx1* in this region as we have previously shown in the head mesenchyme (Yamagishi et

al., 2003). Nevertheless, given the current data, it is a reasonable hypothesis that the more severe effects on *Tbx1* mesoderm transcript level in $Tbx1^{neo/neo}$ embryos may be due to disruption of an amplifying loop involving forkhead proteins.

We had previously reported a Fox site that was necessary and sufficient to direct *Tbx1* expression in the pharyngeal endoderm and head mesenchyme (Yamagishi et al., 2003). Upon searching for a mesoderm enhancer, we were unable to identify a separate genomic region that was sufficient for *Tbx1* mesoderm expression. However, we had observed on rare occasion that the endoderm and head mesenchyme enhancer could direct very low levels of *Tbx1* expression in the pharyngeal mesoderm (H.Y. and D.S., unpublished). The observation here that the previously reported Fox site was necessary but not sufficient for pharyngeal mesoderm expression suggests that it is a weak but essential enhancer for this domain of expression. Because Fox proteins can be involved in chromatin relaxation events, it is possible that the necessary Fox site affects access to other critical cis elements (Cirillo et al., 2002). We were able to identify a 1.5 kb conserved fragment of genomic DNA that was alone insufficient, but was necessary with the Fox site to confer pharyngeal mesoderm expression. We do not yet know the precise cis element within this region or the trans-acting factor that is necessary to collaborate with the Fox site for this purpose, but it will be an important area of future study. Nevertheless, it is striking that a single Fox site upstream of *Tbx1* is necessary for all of the domains of *Tbx1* expression directed by the 12.8 kb upstream genomic DNA.

Tbx1 regulation of Fgfs in the anterior heart field

Our finding that *Fgf8* was downstream of Tbx1 was consistent with previous reports of a connection between these two genes. In particular, *Fgf8* hypomorphs partially phenocopy *Tbx1* mutants (Abu-Issa et al., 2002; Frank et al., 2002); mice trans-heterozygous for *Tbx1* and *Fgf8* have more severe aortic arch defects than either alone (Vitelli et al., 2002); *Fgf8* has been reported to be downregulated in the pharyngeal endoderm of *Tbx1* mutants; and tissue-specific deletion of *Fgf8* in the Tbx1 expressing domain results in cardiac outflow tract defects (Brown et al., 2004). The *Fgf8* enhancer we described is the first in vivo regulatory region reported for *Fgf8* and includes an enhancer that directs *Fgf8* expression in cardiac outflow tract cells derived from the anterior heart field. An *Fgf8* intronic region regulated by engrailed and Pbx1 was previously reported to have activity in vitro and in embryoid bodies, but its ability to regulate activity in vivo in specific domains had not been studied (Gemel et al., 1999). In our hands, the intronic enhancer was not sufficient to direct expression of *lacZ* in transgenic mice.

The observation of outflow tract expression directed by the *Fgf8* enhancer was interesting but unexpected, and led to more careful detection of Fgf8 transcripts in the outflow tract by in situ hybridization. Still, we considered whether this domain of expression for the enhancer may represent outflow tract-specific expression of the neighboring gene *Npm3*. However, this is unlikely because of the ubiquitous expression pattern of *Npm3* (MacArthur and Schackleford, 1997). Consistent with our data is the observation that *lacZ* knocked into the *Fgf8* locus is also expressed in the cardiac outflow tract (E. Meyers,

personal communication). In the *Tbx1* mutant background, this enhancer was not fully activated, suggesting that *Fgf8* requires Tbx1 for regulation in the outflow tract. Together, the evidence supports an interpretation that there are normally low levels of *Fgf8* transcripts in the cardiac outflow tract and that the enhancer described normally directs gene transcription in this domain in a Tbx1-dependent fashion.

Somewhat surprisingly, we did not observe any downregulation of *Fgf8* in the pharyngeal endoderm, as previously reported. This is consistent with the observation that deletion of Fgf8 only in the pharyngeal endoderm or ectoderm does not cause cardiac outflow tract defects (Macatee et al., 2003). Thus, while Tbx1 and Fgf8 do appear to be in common pathways, their collaboration may be most important in the cardiac outflow tract rather than endoderm. Unfortunately, we have been unable to definitively determine if *Fgf8* is a direct target of Tbx1 in vivo. There are at least five predicted core Tbx-binding sequences in the 0.9 kb enhancer of *Fgf8* (see Materials and methods for sequences) and mutation of each individually did not affect *lacZ* expression in transgenic mice nor did tandem mutation of up to three of the sites (T.H. and D.S., unpublished). Although *Fgf8* may indeed be a direct target of Tbx1, convincing in vivo evidence remains elusive.

Finally, a role for Tbx1 regulation of anterior heart field/cardiac outflow tract gene expression was demonstrated by misexpressing *Tbx1* in cardiomyocytes that do not normally express *Tbx1*. By doing so, we found that *Fgf10*, a marker of the anterior heart field, was upregulated and the outflow tract appeared elongated. This could be due to Tbx1-mediated upregulation of *Fgf10* in the ventricular myocytes, or a result of conversion of ventricular myocytes into cells more characteristic of the outflow tract that are derived from the anterior heart field. Although it is difficult to discern between these possibilities, it is clear that Tbx1 plays an essential role in the cardiac outflow tract and, together with its role in the pharyngeal mesoderm, makes it a likely regulator of cardiomyocytes derived from the anterior heart field.

Note added in proof

After submission of this article, a related was published that also demonstrates the dose sensitivity of the Tbx1 allele (Xu et al., 2004).

References

Abu-Issa, R., Smyth, G., Smoak, I., Yamamura, K. and Meyers, E. N. (2002). Fgf8 is required for pharyngeal arch and cardiovascular development in the mouse. *Development* **129**, 4613-4625.

Ang, S. L. and Rossant, J. (1994). HNF-3 beta is essential for node and notochord formation in mouse development. *Cell* **78**, 561-574.

Biben, C., Hatzistavrou, T. and Harvey, R. P. (1998). Expression of NK-2 class homeobox gene Nkx2-6 in foregut endoderm and heart. *Mech. Dev.* **73**, 125-127.

Brown, C. B., Wenning, J. M., Lu, M. M., Epstein, D. J., Meyers, E. N. and Epstein, J. A. (2004). Cre-mediated excision of Fgf8 in the Tbx1 expression domain reveals a critical role for Fgf8 in cardiovascular development in the mouse. *Dev. Biol.* **267**, 190-202.

Cai, C. L., Liang, X., Shi, Y., Chu, P. H., Pfaff, S. L., Chen, J. and Evans, S. (2003). Isl1 identifies a cardiac progenitor population that proliferates prior to differentiation and contributes a majority of cells to the heart. *Dev. Cell* **5**, 877-889.

Chapman, D. L., Garvey, N., Hancock, S., Alexiou, M., Agulnik, S. I., Gibson-Brown, J. J., Cebra-Thomas, J., Bollag, R. J., Silver, L. M. and Papaioannou, V. E. (1996). Expression of the T-box family genes, Tbx1-Tbx5, during early mouse development. *Dev. Dyn.* **206**, 379-390.

Cirillo, L. A., Lin, F. R., Cuesta, I., Friedman, D., Jarnik, M. and Zaret, K. S. (2002). Opening of compacted chromatin by early developmental transcription factors HNF3 (FoxA) and GATA-4. *Mol. Cell* **9**, 279-289.

Conlon, F. L., Fairclough, L., Price, B. M., Casey, E. S. and Smith, J. C. (2001). Determinants of T box protein specificity. *Development* **128**, 3749-3758.

Crossley, P. H. and Martin, G. R. (1995). The mouse Fgf8 gene encodes a family of polypeptides and is expressed in regions that direct outgrowth and patterning in the developing embryo. *Development* **121**, 439-451.

Epstein, J. A. (2001). Developing models of DiGeorge syndrome. *Trends Genet.* **17**, S13-S17.

Frank, D. U., Fotheringham, L. K., Brewer, J. A., Muglia, L. J., Tristani-Firouzi, M., Capecchi, M. R. and Moon, A. M. (2002). An Fgf8 mouse mutant phenocopies human 22q11 deletion syndrome. *Development* **129**, 4591-4603.

Garg, V., Yamagishi, C., Hu, T., Kathiriya, I. S., Yamagishi, H. and Srivastava, D. (2001). Tbx1, a DiGeorge syndrome candidate gene, is regulated by sonic hedgehog during pharyngeal arch development. *Dev. Biol.* **235**, 62-73.

Gemel, J., Jacobsen, C. and MacArthur, C. A. (1999). Fibroblast growth factor-8 expression is regulated by intronic engrailed and Pbx1-binding sites. *J. Biol. Chem.* **274**, 6020-6026.

Graham, A. (2003). Development of the pharyngeal arches. *Am. J. Med. Genet.* **119**, 251-256.

Graham, A. and Smith, A. (2001). Patterning the pharyngeal arches. *Bioessays* **23**, 54-61.

Jerome, L. A. and Papaioannou, V. E. (2001). DiGeorge syndrome phenotype in mice mutant for the T-box gene, Tbx1. *Nat. Genet.* **27**, 286-291.

Kelly, R. G., Brown, N. A. and Buckingham, M. E. (2001). The arterial pole of the mouse heart forms from Fgf10-expressing cells in pharyngeal mesoderm. *Dev. Cell* **1**, 435-440.

Kothary, R., Clapoff, S., Darling, S., Perry, M. D., Moran, L. A. and Rossant, J. (1989). Inducible expression of an hsp68-lacZ hybrid gene in transgenic mice. *Development* **105**, 707-714.

Kume, T., Jiang, H., Topczewska, J. M. and Hogan, B. L. (2001). The murine winged helix transcription factors, Foxc1 and Foxc2, are both required for cardiovascular development and somitogenesis. *Genes Dev.* **15**, 2470-2482.

Lindsay, E. A. (2001). Chromosomal microdeletions: dissecting del22q11 syndrome. *Nat. Rev. Genet.* **2**, 858-868.

Lindsay, E. A., Botta, A., Jurecic, V., Carattini-Rivera, S., Cheah, Y. C., Rosenblatt, H. M., Bradley, A. and Baldini, A. (1999). Congenital heart disease in mice deficient for the DiGeorge syndrome region. *Nature* **401**, 379-383.

Lindsay, E. A., Vitelli, F., Su, H., Morishima, M., Huynh, T., Pramparo, T., Jurecic, V., Ogunrinu, G., Sutherland, H. F., Scambler, P. J. et al. (2001). Tbx1 haploinsufficieny in the DiGeorge syndrome region causes aortic arch defects in mice. *Nature* **410**, 97-101.

Lu, J. R., Bassel-Duby, R., Hawkins, A., Chang, P., Valdez, R., Wu, H., Gan, L., Shelton, J. M., Richardson, J. A. and Olson, E. N. (2002). Control of facial muscle development by MyoR and capsulin. *Science* **298**, 2378-2381.

MacArthur, C. A. and Shackleford, G. M. (1997). Npm3: a novel, widely expressed gene encoding a protein related to the molecular chaperones nucleoplasmin and nucleophosmin. *Genomics* **42**, 137-140.

Macatee, T. L., Hammond, B. P., Arenkiel, B. R., Francis, L., Frank, D. U. and Moon, A. M. (2003). Ablation of specific expression domains reveals discrete functions of ectoderm- and endoderm-derived FGF8 during cardiovascular and pharyngeal development. *Development* **130**, 6361-6374.

Merscher, S., Funke, B., Epstein, J. A., Heyer, J., Puech, A., Lu, M. M., Xavier, R. J., Demay, M. B., Russell, R. G., Factor, S. et al. (2001). TBX1 is responsible for cardiovascular defects in velo-cardio-facial/DiGeorge syndrome. *Cell* **104**, 619-629.

Meyers, E. N. and Martin, G. R. (1999). Differences in left-right axis pathways in mouse and chick: functions of FGF8 and SHH. *Science* **285**, 403-406.

Meyers, E. N., Lewandoski, M. and Martin, G. R. (1998). An Fgf8 mutant allelic series generated by Cre- and Flp-mediated recombination. *Nat. Genet.* **18**, 136-141.

Mjaatvedt, C. H., Nakaoka, T., Moreno-Rodriguez, R., Norris, R. A., Kern, M. J., Eisenberg, C. A., Turner, D. and Markwald, R. R. (2001). The outflow tract of the heart is recruited from a novel heart-forming field. *Dev. Biol.* **238**, 97-109.

Muller, T. S., Ebensperger, C., Neubuser, A., Koseki, H., Balling, R., Christ, B. and Wilting, J. (1996). Expression of avian Pax1 and Pax9 is intrinsically regulated in the pharyngeal endoderm, but depends on environmental influences in the paraxial mesoderm. *Dev. Biol.* **178**, 403-417.

Scambler, P. J. (2000). The 22q11 deletion syndromes. *Hum. Mol. Genet.* **9**, 2421-2426.

Schinke, M. and Izumo, S. (2001). Deconstructing DiGeorge syndrome. *Nat. Genet.* **27**, 238-240.

Shaikh, T. H., Kurahashi, H. and Emanuel, B. S. (2001). Evolutionarily conserved low copy repeats (LCRs) in 22q11 mediate deletions, duplications, translocations, and genomic instability: an update and literature review. *Genet. Med.* **3**, 6-13.

Thomas, T., Kurihara, H., Yamagishi, H., Kurihara, Y., Yazaki, Y., Olson, E. N. and Srivastava, D. (1998). A signaling cascade involving endothelin-1, dHAND and msx1 regulates development of neural-crest-derived branchial arch mesenchyme. *Development* **125**, 3005-3014.

Vitelli, F., Taddei, I., Morishima, M., Meyers, E. N., Lindsay, E. A. and Baldini, A. (2002). A genetic link between Tbx1 and fibroblast growth factor signaling. *Development* **129**, 4605-4611.

Waldo, K. L., Kumiski, D. H., Wallis, K. T., Stadt, H. A., Hutson, M. R., Platt, D. H. and Kirby, M. L. (2001). Conotruncal myocardium arises from a secondary heart field. *Development* **128**, 3179-3188.

Weinstein, D. C., Ruiz i Altaba, A., Chen, W. S., Hoodless, P., Prezioso, V. R., Jessell, T. M. and Darnell, J. E., Jr (1994). The winged-helix transcription factor HNF-3 beta is required for notochord development in the mouse embryo. *Cell* **78**, 575-588.

Winnier, G. E., Kume, T., Deng, K., Rogers, R., Bundy, J., Raines, C., Walter, M. A., Hogan, B. L. and Conway, S. J. (1999). Roles for the winged helix transcription factors MF1 and MFH1 in cardiovascular development revealed by nonallelic noncomplementation of null alleles. *Dev. Biol.* **213**, 418-431.

Xu, H., Morishima, M., Wylie, J. N., Schwartz, R. J., Bruneau, B. G., Lindsay, E. A. and Baldini, A. (2004). Tbx1 has a dual role in the morphogenesis of the cardiac outflow tract. *Development* **131**, 3217-3227.

Yamagishi, H. and Srivastava, D. (2003). Unraveling the genetic and developmental mysteries of 22q11 deletion syndrome. *Trends Mol. Med.* **9**, 383-389.

Yamagishi, H., Maeda, J., Hu, T., McAnally, J., Conway, S. J., Kume, T., Meyers, E. N., Yamagishi, C. and Srivastava, D. (2003). Tbx1 is regulated by tissue-specific forkhead proteins through a common Sonic hedgehog-responsive enhancer. *Genes Dev.* **17**, 269-281.

Yutzey, K. E. and Kirby, M. L. (2002). Wherefore heart thou? Embryonic origins of cardiogenic mesoderm. *Dev. Dyn.* **223**, 307-320.